Article citation info:
Jiang L.: Construction and application of a bearing fault diagnosis model based on improved GWO algorithm. Diagnostyka, 2024;25(3):2024302. https://doi.org/10.29354/diag/189904.

DIAGNOSTYKA, 2024, Vol. 25, No. 3

e-ISSN 2449-5220
DOI: 10.29354/diag/189904

CONSTRUCTION AND APPLICATION OF A BEARING FAULT DIAGNOSIS MODEL BASED ON IMPROVED GWO ALGORITHM

Lingbo JIANG

School of Mechanical and Electronic Engineering, Shandong Vocational College of Industry, Zibo 256414, China
Corresponding author, e-mail: jianglb2021@163.com

Abstract

In mechanical equipment, if bearing components fail, it can cause serious equipment damage and even threaten human life safety. Therefore, equipment bearings fault diagnosis is of great meaning. In the study of bearing fault diagnosis, an improved gray wolf optimization algorithm is put forward to optimize the support vector machine model. The model improves the convergence factor of the algorithm, and then optimizes the penalty factor and KF parameters of the support vector machine to enhance the accuracy of fault classification. At the same time, in the problem of fault identification, the introduction of adaptive noise set empirical mode decomposition and the combination of permutation entropy are studied to minimize the impact of noise on the identification model. The experimental outcomes indicated that the algorithm proposed in the study had an average fitness value and a standard deviation fitness value of 0 in the benchmark test function and 94.55% accuracy in overall fault identification. The permutation entropy of the vibration signal in the normal state of the bearing was within the range of [0.13, 0.52], which has a more stable state compared to the fault state. The results show that the improved grey Wolf optimization algorithm is applied to the optimization of support vector machine, combined with the adaptive noise set empirical mode decomposition and permutation entropy, and the identification and classification results of bearing faults are successfully improved, making the proposed method feasible in bearing fault diagnosis, and providing a more effective scheme for fault diagnosis.

Keywords: Grey wolf optimization algorithm, support vector machine, bearings, fault, permutation entropy

List of Symbols/Acronyms
BFD – Bearing Fault Diagnosis,
BFs – Bearing Faults,
DBN –Deep Belief Network,
DSOGIFLL– Generalized Integrator with Frequency Locked Loop,
GA – Genetic Algorithm,
GWO – Grey Wolf Optimization,
ICEEMDAN – Improve Complete Ensemble Empirical Mode Decomposition with Adaptive Noise,
IMF – Instant Mode Function,
KF – Kernel Function,
KMGWO – K-means Clustering Grey Wolf Optimization,
LSSVR– Least Squares Support Vector Regression,
PE– Permutation Entropy,
PSO – Particle Swarm Optimization,
SCA– Sine Cosine Algorithm,
SVM – Support Vector Machines,

1. INTRODUCTION

Bearings are a widely used component in contemporary mechanical equipment, which is mainly used to limit relative motion to only allow the desired motion, reduce friction and support rotating parts. In operation, the bearing bears loads from different directions, and if a failure occurs, it will cause increased friction and may even lead to damage to mechanical equipment [1]. Therefore, accurate Bearing Fault Diagnosis (BFD) is very important. However, due to the complexity and diversity of bearing working conditions, as well as the uncertainty of environmental conditions, BFD has become a nonlinear and non-stationary problem [2]. Currently, traditional methods have limitations in dealing with such nonlinear and non-stationary problems, leading to often unsatisfactory diagnostic results. With the development of science and technology, more and more methods have been put forward for BFD, especially intelligent algorithms play an important role in it. Neural networks, support vector machines (SVM), deep learning, etc., have been widely used in this field in recent years. These methods are particularly suitable for nonlinear and non-stationary feature recognition tasks because they are able to identify underlying patterns and trends from complex data. But they require large-scale training data, and the training and optimization process often consumes a large amount of computing resources [3-4]. Furthermore, with the goal of solving this problem, an improved Grey Wolf

Received 2024-02-03; Accepted 2024-06-11; Available online 2024-07-11

Optimization (GWO) algorithm-based fault diagnosis model for optimizing SVM was raised. This model improved the GWO algorithm's convergence factor, and then optimized the penalty factor and kernel function (KF) parameters of the SVM. In the study of fault identification problems, Improve Complete Ensemble Empirical Mode Decomposition with Adaptive Noise (ICEEMDAN) was raised and combined with permutation entropy (PE) to minimize the influence of noise on the identification model and make fault diagnosis outcomes more accurate. The main innovation of the research lies in the usage of the improved GWO algorithm to the optimization of SVMs for the first time. And combined with ICEEMDAN and PE, it can successfully improve the recognition and classification results of bearing faults (BFs). This new type of fault diagnosis method not only performs well in handling complex and non-stationary BF identification problems, but also significantly improves the accuracy of fault classification. The contribution of the research mainly contains two aspects: firstly, a novel and effective BFD method has been proposed. Secondly, this method has certain advantages in BF identification and classification, and has the potential to handle nonlinear and non-stationary problems. The research structure mainly includes four parts. The first part summarizes the research results of domestic and foreign scholars on the GWO algorithm and BFD. The second part is to construct an improved GWO-SVM BFD model, and further optimize the model by introducing ICEEMDAN and PE. The third part is to conduct performance and comparison analysis of the constructed model. The final part summarizes the performance status of the model, analyzes the shortcomings in the research, and points out future research directions.

2. RELATED WORKS

As the continuous growth of intelligent technology, the GWO algorithm has gradually been mentioned and improved in fault identification problems, and many domestic and foreign scholars have conducted research and analysis on the GWO algorithm. Diab et al. conducted research on variants of the GWO algorithm to evaluate the unknown parameters of the proton exchange membrane fuel cell model. And the also applied the algorithm to three commercial proton exchange membrane fuel cell stacks to calculate the sum of squared errors based on parameter estimation results and experimental testing results. Through simulation results, the improved GWO algorithm could promote the optimization efficiency of the 250 W heap to 99.97 [5]. Yang et al. proposed a combined algorithm based on the Sine Cosine Algorithm (SCA) and GWO algorithm to optimize the regression prediction model of the Least Squares Support Vector Regression (LSSVR) algorithm. This method used an improved GWO algorithm to search the population to get the optimal least squares support vector machine parameter solution. The experiment findings illustrated that this method's fitting accuracy reached 86.8%, which improved the fitting accuracy by 5% compared to the original model [6]. Mohammed et al. conducted research on GWO algorithms with the main aim of enhancing the limitations of the search process for wolf packs attacking gray wolves. The study uses the K-means clustering algorithm to strengthen the effectiveness of the original GWO, and the novel algorithm is named the K-means Clustering Gray Wolf Optimization (KMGWO) algorithm. The survey outcomes indicate that KMGWO has a higher efficiency improvement compared to GWO. To assess the effectiveness of KMGWO, it was utilized to solve the CEC2019 benchmark test function, and its performance was better than other meta heuristic algorithms [7]. Doumbia et al. introduced a direct power control technology based on instantaneous power theory, which uses the GWO algorithm to optimize the PI controller. This method allowed for the control of active and reactive power and improved the quality of the generated electricity. A Dual Second-order Generalized Integrator with Frequency Locked Loop (DSOGI-FLL) was used to ensure grid synchronization. A new objective function was defined and the optimization process was executed using the GWO. A simulation study was conducted on the grid connected system based on three-phase inverters. The superiority of the new method has been demonstrated through analysis and comparative research on different operating modes [8].

In fault identification and diagnosis, scholars have proposed many different methods for performance verification. Chen et al. proposed a new simple and effective deep attention mechanism network that combines channel and spatial attention mechanisms, and residual structure. The nonlinear transformation layer was a soft threshold function and extended convolution was introduced to build a dual path neural network. Then, important features in the signal could be selected without the use of any signal denoising algorithm. The outcomes indicated that this method can greatly promote the fault diagnosis accuracy [9]. The Gao team proposed an innovative optimized adaptive deep belief network (DBN) and used it to solve the issue of rolling BF identification. DBN was optimized using the intelligent optimization method salp swarm algorithm. Finally, simulations on the ground of experiment data evidenced this method's effect [10]. Tao et al. proposed an unsupervised cross-domain fault diagnosis method. The wavelet packet decomposed and reconstructed the bearing's vibration signal, as well as the energy feature vector to obtain a two-dimensional time-frequency map of the fault features. The model was used to motor bearings for comparative verification. The outcomes indicated that this method had high diagnostic accuracy and strong robustness [11]. Cui et al. first

proposed unsupervised learning to understand data attributes, followed by sensitivity analysis to extract significant features and avoid overfitting. In this process, segmented attributes were learned to improve supervised learning. A three-stage learning algorithm was raised to extract and study the most significant information for turbine BFD. The raised framework was proved by using real data from various datasets of bearing non-stationary vibration signals [12].

In summary, many manners have been used in BFD. Although these methods have achieved certain improvement results in experiments, there is still room for improvement in their methods, such as algorithm complexity, computational speed, recognition accuracy, and other issues. Recently, the GWO algorithm has also been gradually mentioned in the fault diagnosis neighborhood, which has a simple structure, fast computation speed, and strong stability. Therefore, based on the GWO algorithm, ICEEMDAN and PE are introduced to improve the algorithm, with the aim of further improving model performance and reducing the influence of noise on the model.

3. CONSTRUCTION OF A BFD MODEL BASED ON IMPROVED GWO ALGORITHM

BFD plays a crucial role in the operation and maintenance of large equipment and machinery, which can avoid sudden faults and damage to the equipment. BFD has high complexity, and the occurrence of faults is characterized by diversity and strong nonlinearity. The fault signal is easily affected by noise, which increases the difficulty of BFs. To solve the problem of BFD, an improved GWO algorithm-based diagnostic model is proposed. The model classifies BFs using SVM and identifies faults using the improved GWO algorithm.

3.1. Bearing fault classification model based on SVM

SVM is a widely used supervised learning model for data classification and regression analysis, which has good generalization performance and is suitable for dealing with high-dimensional and nonlinear complex problems [13-14]. The principle of SVM is to find a hyperplane to separate data points of different categories, as shown in Fig. 1.

In Fig. 1, "circle" and "triangle" represent different data points, where β represents the classification line, and the distance between β_1 and β_2 represents the classification interval. The classification line is described by Eq. (1).

$$\omega x + b = 0 \tag{1}$$

In Eq. (1), ω represents the coefficient of the formula classification line, and b denotes a constant that means the translation position of the classification line. The size of the classification interval in the figure is $2/\|\omega\|$. When the value of $\|\omega\|$ is the smallest, the classification interval is the largest. At this point, SVM transforms the classification problem into a minimum value problem, and during the classification of SVM, the optimal solution is obtained for the parameters. The study introduces Lagrange multipliers in SVM to address the optimization of SVM parameters, and the formula is shown in Eq. (2).

$$L(\omega, b, \alpha) = \frac{1}{2}\|\omega\|^2 - \sum_{i=1}^{n} \alpha_i [y_i[(\omega \cdot x_i) + b] - 1] \tag{2}$$

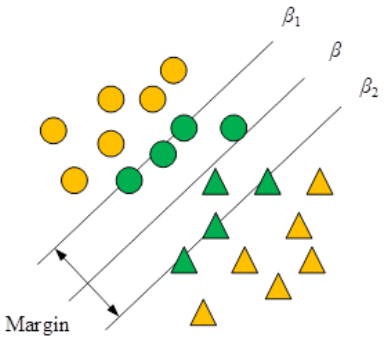

Fig. 1. Principle of SVM classification

In Eq. (2), α_i represents the Lagrange multiplier. L represents taking the derivative of parameters ω, b and α, making the derivative value 0, then there is Eq. (3).

$$max\, L(\omega, b, \alpha) = \sum_{i=1}^{n} \alpha_i - \frac{1}{2}\sum_{i=1}^{n}\sum_{j=1}^{n} \alpha_i \alpha_j y_i y_j (x_i \cdot x_j) \tag{3}$$

Assuming the optimal solution in Eq. (3) is α_i^*, then there is $\omega^* = \sum_{i=1}^{n} \alpha_i^* y_i x_i$, and the corresponding coefficient b^* can be calculated. The optimal classification function is shown in Eq. (4).

$$y = sgn(f(x)) = sgn((\omega^* \cdot x) + b^*) = sgn(\sum_{i=1}^{n} \alpha_i^* y_i (x_i \cdot x) + b^*) \tag{4}$$

The type of most unknown samples can be determined through Eq. (4), but there are still a small number of samples during classification. Therefore, research also needs to introduce fault-tolerant variables, denoted as δ_i, whose main function is to allow for misclassification of samples. The classification expression after introducing fault-tolerant variables is shown in Eq. (5).

$$\begin{cases} min\dfrac{1}{2}\|\omega\|^2 + c\sum_{i=1}^{n}\delta_i \\ y_i[(\omega \cdot x_i) + b] - 1 + \delta_i \end{cases} \quad (5)$$

In Eq. (5), c represents the penalty factor. In real life, many high-dimensional samples have linear and indivisible attributes, making it difficult to directly use SVM for classification. At this point, SVM needs to introduce KFs to solve such problems. The status data is mapped to a high-dimensional space, and the corresponding segmentation is performed in the high-dimensional space. The expression is expressed in Eq. (6) [15].

$$K(x_i, x_j) = \Phi(x_i) \cdot \Phi(x_j) \quad (6)$$

In Eq. (6), $\Phi(x_i)$ means a nonlinear mapping function, which is used to replace Eq. (3) and solve the meta feature space to obtain Eq. (7).

$$\begin{cases} max\, L(\omega, b, \alpha) = \sum_{i=1}^{n}\alpha_i - \dfrac{1}{2}\sum_{i=1}^{n}\sum_{j=1}^{n}\alpha_i\alpha_j y_i y_j(\Phi(x_i)\cdot\Phi(x_j)) \\ y = sgn((\omega^* \cdot \Phi(x)) + b^* = sgn(\sum_{i=1}^{n}\alpha_i^* y_i K(x_i \cdot x) + b^*) \end{cases} \quad (7)$$

From Eq. (7), this method of calculation has no relationship with the data dimension and can classify low-dimensional data as well as solve high-dimensional data. The SVM algorithm constructed above can be used in bearing fault classification, which can effectively process complex feature data and accurately classify bearing states by constructing optimal interface.

3.2. Bearing fault identification based on GWO algorithm

The main reason for implementing the nonlinear mapping function of formula (7) is that SVM introduces KFs, and different KFs have different effects. Common KFs include linear KFs, Gaussian radial basis functions, Sigmoid KFs, and polynomial KFs. Among them, linear KF has fewer parameters and runs faster, but its accuracy in classification solution is poor; The Sigmoid KF is equivalent to a multi-layer neural network in the SVM structure, and its running speed is relatively slow. Polynomial KFs have a large number of parameter codes, high computational complexity, and poor learning ability [16]. Therefore, the radial KF was selected for the study, which has strong local characteristics and has good performance in dealing with nonlinear problems. After studying the classification model for BFD, it now analyzes the BF identification model. In BF identification, the GWO algorithm is mainly used in research [17]. The prototype of this algorithm comes from the social behavior and hunting strategy of gray wolves, which are social animals and their hunting behavior includes searching, approaching, and chasing prey. In the algorithm, the gray wolf simulates these behaviors to find the optimal solution in the solution space. There is a clear social hierarchical structure in the gray wolf population, as shown in Fig. 2.

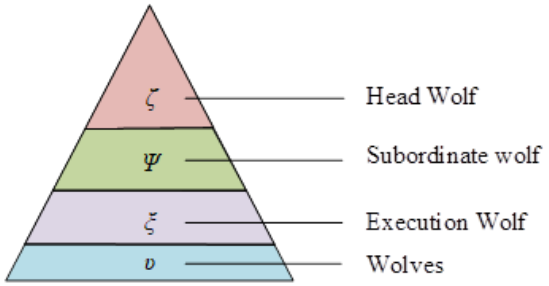

Fig. 2. Social hierarchy structure of wolf packs

Fig. 2 shows the social hierarchy structure of wolf packs, including head wolf, subordinate wolf, executive wolf, and wolf pack, denoted as ζ, ψ, ξ, and υ, respectively. The head wolf is the leader of the pack and has the highest decision-making power. The subordinate wolf is the deputy leader of the wolf pack, and coercing the head wolf to make decisions is its duty. Executive wolf is the complete execution of leader commands to maintain the normal operation of the wolf pack. The wolf pack is responsible for performing search tasks. In the preparation stage of wolf pack hunting, there is no clear prey information when the wolf pack enters the hunting ground, and they can only track their prey by constantly searching for scent. Therefore, during the hunting process, wolf packs of four levels of status need to adjust their positions and constantly approach their prey. In the hunting, the step 1 is to approach the prey, the step 2 is to surround the prey, and the step 3 is to attack the prey. The research conducted data modeling through the above steps. Assuming that the iteration times of the model is t, the position vector of the prey and the wolf pack are denoted as X_p and X, respectively. The linear distance between the prey and the wolf pack can be represented by Eq. (8) [18].

$$D = \left|CX_p(t) - X(t)\right| \quad (8)$$

In Eq. (8), C represents the coefficient vector. After obtaining the distance between the prey and the wolf pack through Eq. (8), the wolf pack adjusts its position as shown in Eq. (9).

$$\begin{cases} X(t+1) = X_p(t) - AD \\ A = 2ar_1 - a \\ C = 2r_2 \\ a = 2 - 2(\dfrac{t}{t_{max}}) \end{cases} \quad (9)$$

In Eq. (9), A represents the coefficient vector. r_1 and r_2 represent random vectors, with values ranging from [0, 1], and a represents the convergence factor, which is inversely proportional to the iteration times. After the head wolf roughly determines the location of the prey, it will lead the subordinate wolf to hunt around the prey. During the hunting, it uses the wolf pack and the prey's location to accurately locate the prey and ultimately complete the attack. The position changes of prey captured by wolf packs can be represented by Eq. (10) [19].

$$\begin{cases} D_\zeta = \left|C_1 X_\zeta(t) - X(t)\right| \\ D_\psi = \left|C_2 X_\psi(t) - X(t)\right| \\ D_\xi = \left|C_3 X_\xi(t) - X(t)\right| \\ X_1 = X_\zeta - A_1 D_\zeta \\ X_2 = X_\psi - A_2 D_\psi \\ X_3 = X_\xi - A_3 D_\xi \end{cases} \tag{10}$$

In Eq. (10), when the vector coefficient $|A|$ is greater than 1, the wolf pack will increase the area of the hunting area and search for prey in a larger range. In the algorithm, global search is performed to increase convergence speed. When $|A|$ is less than 1, the wolf pack reduces the area of the hunting area and determines the position of the prey. In the algorithm, local search is performed to slow down the convergence speed. The GWO algorithm is most likely to fall into local optima when the wolf pack changes its attack direction. Because when changing the attack direction, the prey's position will constantly change, leading to the loss of prey [20]. When a wolf pack seizes its prey, its position update diagram is shown in Fig. 3.

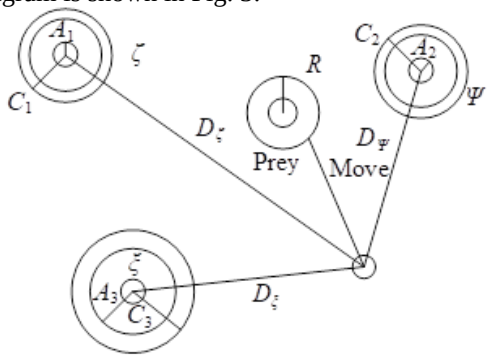

Fig. 3. Schematic diagram of wolf pack encirclement location

3.3. Construction of improved GWO algorithm

The above GWO algorithm is mainly used in BFD to find the optimal parameters or features to achieve the best fault recognition effect. However, GWO also has some limitations, such as parameter selection issues and local optimal traps. To overcome the above limitations, a method, ICEEMDAN, is introduced. The principle of this method is to add adaptive white noise during the decomposition process, and the reconstructed signal after decomposition is almost the same as the original signal. This method improves the residual noise problem of the Intrinsic Mode Function (IMF) component to some extent. ICEEMDAN adds paired positive and negative Gaussian white noise to the initial signal before decomposing it, as shown in Eq. (11).

$$x^{(i)} = x + o_k v^{(i)} \tag{11}$$

In Eq. (11), o_k represents the standard deviation of noise, and $v^{(i)}$ represents paired positive and negative Gaussian white noise. The residual value between the first modal component and the modal component of ICEEMDAN is shown in Eq. (12).

$$\begin{cases} IMF_1 = \dfrac{1}{N}\sum_{j=1}^{1} E_1[x^{(j)}] \\ R_1 = x - IMF_1 \end{cases} \tag{12}$$

In Eq. (12), E represents the IMF obtained through decomposition. Positive and negative Gaussian white noise are added to the residual in Eq. (12) to obtain a new signal. By performing the same processing on the new signal, the second modal component and the residual of the modal component can be obtained. This repetition can effectively solve the problem of modal overlap during decomposition, but residual noise will still be retained. Therefore, the study combines PE with ICEEMDAN, which is an information entropy with advantages such as simple calculation and strong noise resistance. PE can accurately describe complex time series mutations and has strong sensitivity to dynamic data. Its expression is shown in Eq. (13).

$$\begin{cases} X_1 = \{x(1), x(1+T), \ldots, x(1+(m-1)T)\} \\ X_2 = \{x(2), x(2+T), \ldots, x(2+(m-1)T)\} \\ \ldots \\ X_k = \{x(k), x(k+T), \ldots, x(k+(m-1)T)\} \end{cases} \tag{13}$$

In Eq. (13), m refers to the embedding dimension, and T means the delay time. There are $m!$ ways to arrange the reconstructed components in ascending order. At this point, the probability distribution of the position sequence is calculated as shown in Eq. (14).

$$\sum_{j=1}^{n} P_j = 1 \tag{14}$$

In Eq. (14), P represents the probability of the position sequence. Therefore, the PE of time series is defined as Eq. (15).

$$PE(y) = -\sum_{T-1}^{m!} P(\pi_{j_1 j_2 \ldots j_m}) \ln P(\pi_{j_1 j_2 \ldots j_m}) \tag{15}$$

In Eq. (15), π represents the arrangement pattern of the reconstructed vector. When $P(\pi_{j_1 j_2 \ldots j_m}) = 1/m!$ is satisfied, the maximum value $ln(m!)$ will be obtained. Based on the analysis of the overview, the process of using the improved model in BFD is shown in Fig. 4.

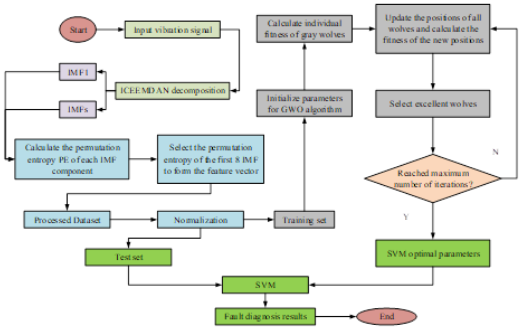

Fig. 4. Flow chart of BFD for ICEEMDAN-PE

4. PERFORMANCE ANALYSIS OF A BFD MODEL BASED ON IMPROVED GWO ALGORITHM

To evidence the proposed method's feasibility, the performance of the model was analyzed through simulation and comparative experiments. The experiment used bearing data from a certain university for simulation analysis. The research used benchmark testing functions and BF examples to verify the research method's effectiveness, and used fitness values, fault decomposition values, recognition accuracy, etc. as algorithm performance evaluation indicators.

4.1. Performance testing of improved GWO algorithm

The experimental data adopted the fault data of the drive end, and deep groove ball bearing 6406 was applied as the analysis object. The data set includes normal bearing, inner ring failure, outer ring failure and rolling element failure. Among them, normal bearings have no signs of failure and can be used as control group to identify fault characteristics. The inner ring failure is simulated by creating a groove of a specific size in the inner ring, for example 1mm width and 0.5mm depth; The outer ring fault is to design a groove of the same size in the outer ring to imitate the situation of the outer ring peeling; The fault of rolling element is to design grooves on the rolling element to simulate the damage of the rolling element. The motor speed was set at 1800 r/min, the sampling frequency was set at 12 Hz, and the load was set at 0HP. The three-dimensional structure of the model was established through Solid Works in the experiment, and simulation analysis was conducted through COMSOL. A rectangular groove with a width of 1mm and a depth of 0.5mm was built to simulate the peeling fault of the rolling bearing. The outer ring fault model and the rotor system model of the rolling bearing test bench constructed are denoted in Fig. 5.

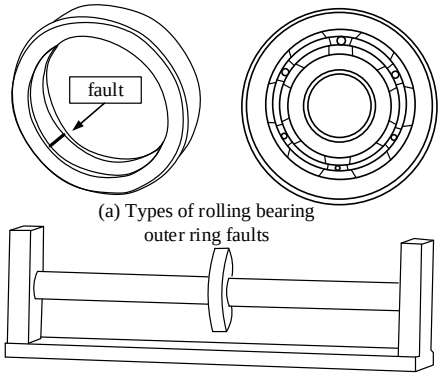

(a) Types of rolling bearing outer ring faults

(b) Model of rotor system for rolling bearing test bench

Fig. 5. Three-dimensional structure of rolling bearings

To validate the performance of the improved GWO algorithm, two benchmark test functions were used for experiments. Simultaneously it selected genetic algorithm (GA), particle swarm optimization (PSO), GWO algorithm, and the ICEEMDAN-PE algorithm proposed in the study for comparative experiments. The benchmark functions selected for the study were unimodal testing function and multimodal testing function, as shown in Fig. 6.

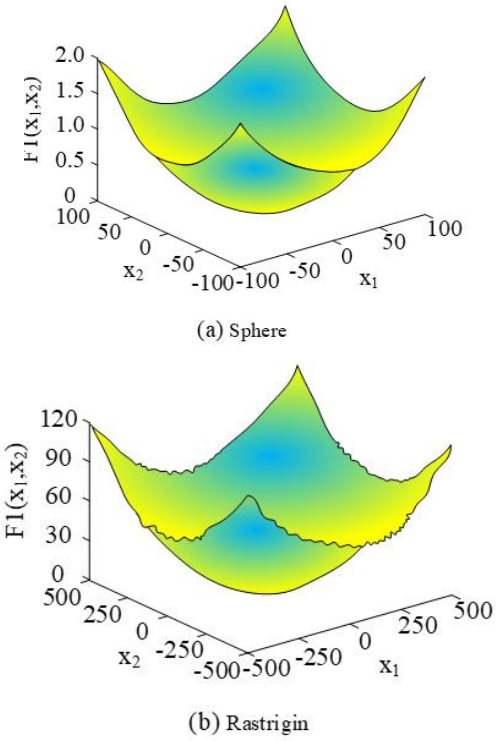

(a) Sphere

(b) Rastrigin

Fig. 6. Reference test function hole

Fig. 6(a) represents the Sphere function, which is a classic benchmark function commonly utilized to assess the effectiveness of intelligent algorithms. Fig. 6(b) represents the Rastigin function, which has multiple local optima and poses certain difficulties in finding a global optimal solution. This test function aims to prove whether the algorithm can jump out of the local optimal solution. According to the benchmark test function mentioned above, the mean fitness and standard deviation fitness values of the comparison algorithm are denoted in Table 1.

From Table 1, the average fitness value of the ICEEMDAN-PE algorithm in the Rastigin function was 0, indicating that the method found the global optimal solution in the function. In the Sphere function, although the ICEEMDAN-PE algorithm did not have a global optimal solution, its optimization performance was significantly improved compared to other algorithms. In terms of standard deviation fitness, the ICEEMDAN-PE algorithm still had a Rastigin function of 0, indicating that the method found the global optimal solution in the function and had the highest stability. In the Sphere function, the ICEEMDAN-PE algorithm had better stability compared to other algorithms. The results indicated that the optimization ability and stability of the improved algorithm model have been effectively raised.

Table 1. Comparison of algorithm mean fitness and standard deviation fitness values results

Average fitness				
Name	GA	PSO	GWO	ICEEMDAN-PE
Sphere function	2.06E-05	7.30E-09	9.56E-28	1.98E-41
Rastigin function	3.85	6.68	1.83E-12	0
Standard deviation fitness				
Name	GA	PSO	GWO	ICEEMDAN-PE
Sphere function	4.99E-05	1.19E-08	1.41E-27	3.71E-41
Rastigin function	2.41	4.13	1.12E-11	0

4.2. Example analysis of BFD

The study divided the BF states in the dataset into four types: normal bearing, rolling element fault, inner and outer ring fault. 50 sets of samples were chosen for each fault state, with 2048 sampling data points per set. The time-domain waveform of the bearing state is expressed in Fig. 7.

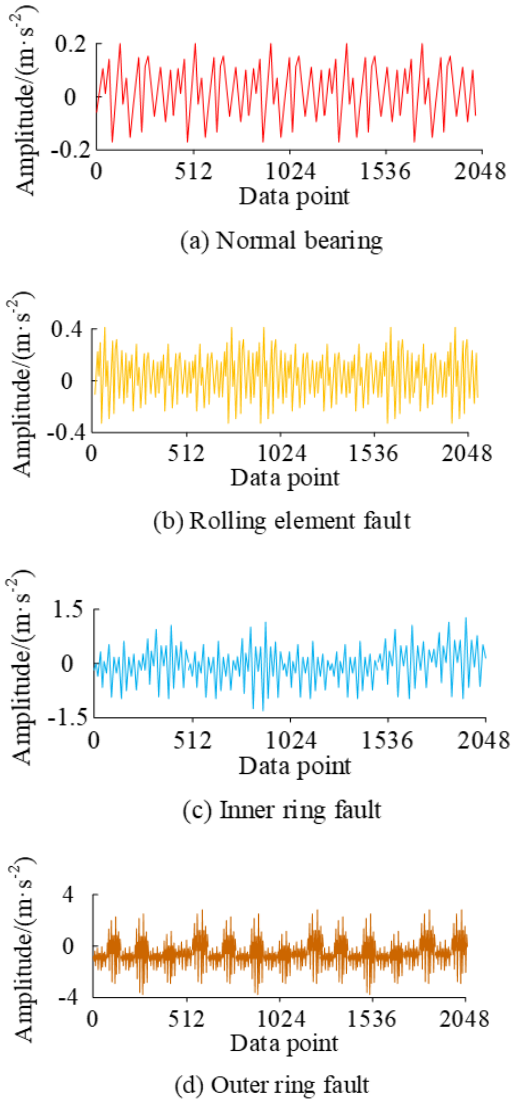

Fig. 7. Time domain waveform of bearing state

At the same time, the CEEMDAN model and ICEEMDAN-PE model were used to compare the decomposition results. The model noise's standard deviation was set to 0.2, the average amount of experiments was 100, and the max amount of iterations was 1000. The decomposition results of the two models for rolling element faults are shown in Fig. 8.

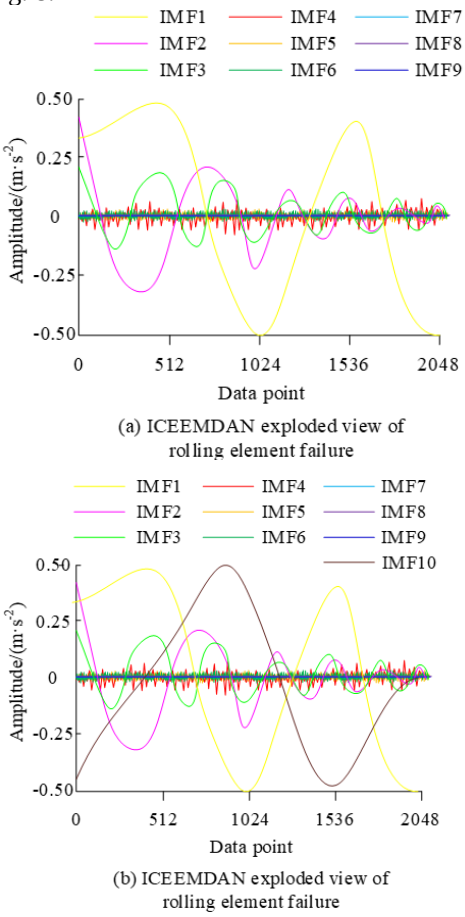

Fig. 8. Decomposition diagram of rolling element faults using different algorithms

Fig. 8(a) shows the rolling element fault decomposition diagram of the CEEMDAN model, where the original signal was decomposed into 10 IMF and one residual component. Fig. 8(b) shows the rolling fault decomposition diagram of the ICEEMDAN-PE model, where the original signal was decomposed into 9 IMF and one residual component. Comparing the two figures, the ICEEMDAN-PE model was more complete and simple, mainly reducing the modal aliasing phenomenon that occurred during the signal decomposition process. The results show that the ICCEMDAN-PE algorithm has significant performance advantages in solving optimization problems, can locate the global optimal solution reliably, and shows high consistency and accuracy in the repeated running of the algorithm. The study represented four types of BF states using labels 1-4 and classified BFs using the model. The results are shown in Fig. 9.

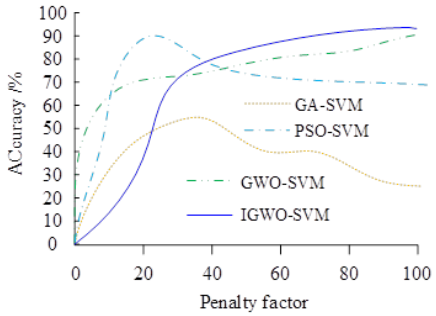

Fig. 9. Classification results of bearing faults

In Fig. 9, GA-SVM, PSO-SVM, GWO-SVM, and IGWO-SVM models were used for comparative experiments. Fig. 9 shows the results of GA-SVM. The optimal parameter of the model was 38.7736, the optimal parameter was 0.240324, and the overall fault classification accuracy was 55.27%. Fig. 9 shows the PSO-SVM results, with of 100 and of 0.716302. The overall fault classification accuracy was 89.99%; Fig. 9 shows the GWO-SVM results, with a of 24.139 and a of 0.452834. The overall fault classification accuracy was 92.78%. Fig. 9 shows the IGWO-SVM results, with being 97.5163 and being 0.136261. The overall fault classification accuracy was 94.55%. The bearing fault classification results in Fig. 9 show that the IGWO-SVM model integrated with ICCEMDAN shows the best fault classification accuracy, because the signals processed by ICCEMDAN can better highlight fault related features, and the GWO algorithm improves the accuracy of SVM parameter selection. The study selected bearing vibration signals in four different states to analyze the PE results after model decomposition, with a time delay of 2 and an embedding dimension of 3. The specific results are shown in Fig. 10.

In Fig. 10, the PE values of the four states exhibited a certain pattern. Under the same sample size, the PE values of the four states all increased with the increase of IMF number, with the most obvious state being the normal state of the bearing; Under the same number of IMF, the PE values of the four states have no relationship with the sample size, and their values are relatively stable. The results show that under the same sample size, the PE value of bearings in normal state is relatively stable, while the PE value of bearings in fault state increases with the increase of the number of IMF, especially the change of normal state is the most obvious. For different IMF quantities, PE values in the four states are relatively stable, which means that PE values can be used as a robust feature for classification. To understand the eigenvector values of specific PE, the PE eigenvectors of bearing vibration signals are described in Table 2 in the experiment.

Table 2. PE eigenvector values of different bearing vibration signals

Bearing status	PE eigenvector			
	IMF-1	IMF-2	IMF-3	IMF-4
Normal	0.5140	0.3678	0.2113	0.2215
Rolling element fault	0.4161	0.8624	0.6332	0.6443
Inner ring failure	0.5342	0.3985	0.2179	0.1927
Outer ring fault	0.4042	0.8659	0.6738	0.6779
Bearing status	PE eigenvector			
	IMF-5	IMF-6	IMF-7	IMF-8
Normal	0.1349	0.1985	0.3157	0.4346
Rolling element fault	0.5648	0.5617	0.6019	0.5969
Inner ring failure	0.1380	0.2208	0.3313	0.4377
Outer ring fault	0.5928	0.5957	0.6103	0.5807

In Table 2, the study selected the first 8-order IMF as the fault characteristic components of the vibration signals in each state. From data analysis, the vibration signal of bearings in normal state was more stable, and its PE eigenvector value was in the range of [0.13, 0.52]. The PE eigenvector values of rolling graph faults were within the range of [0.41, 0.87]. The PE eigenvector values of faults within the circle were within the range of [0.13, 0.54]. The PE eigenvector values of out of circle faults were within the range of [0.40, 0.87]. The results indicated that the fluctuation of the PE eigenvectors of the three

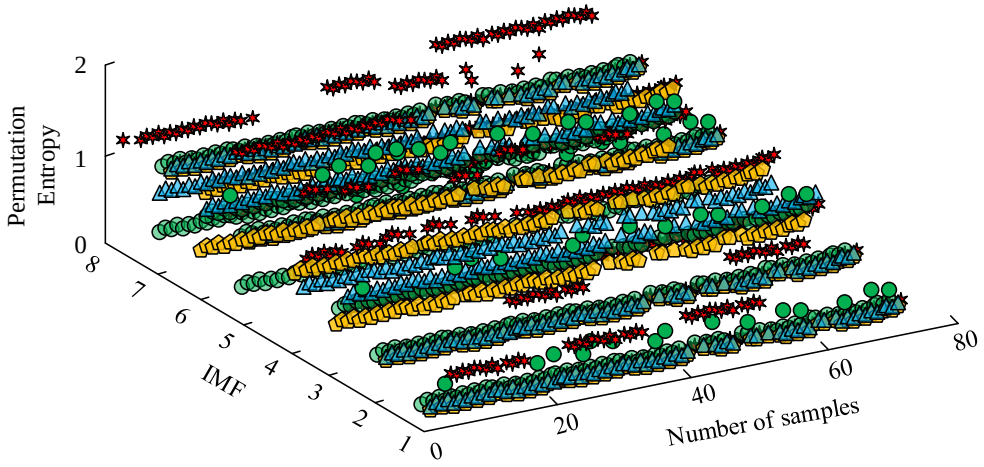

Fig. 10. PE results of various components of bearing vibration signal

fault states increased, indicating good discrimination.

5. CONCLUSION

As one of the important components of mechanical equipment, the failure of bearings can have a serious impact on equipment, work, and life. Therefore, research was conducted on the identification and classification of BF states. A GWO-SVM model combining ICEEMDAN-PE was proposed in this study. The model utilized ICEEMDAN-PE to analyze BF signals and obtain vibration signals under different fault states, which are used to optimize the differentiation of BF states. Research applied improved GWO algorithm to optimize SVM, adjust the parameter settings of SVM, and achieve more accurate classification of BF types. The performance analysis of the model was conducted through simulation and comparative experiments. The research outcomes denoted that the mean fitness and standard deviation fitness values of the ICEEMDAN-PE algorithm in the Sphere function and Rastigin function were both 0. The IGWO-SVM model had an overall fault classification accuracy of 94.55%. The PE eigenvector of bearing vibration signals had obvious discrimination. The experimental results verified the superiority of this model in BF identification and its excellent effectiveness in processing nonlinear and non-stationary signals, providing a powerful tool for future machine health monitoring and fault diagnosis. However, there are still shortcomings in the research, as the test data in the study was mainly based on specific BF types and datasets. If it is applied to more complex or different types of faults, the effectiveness of this method may vary. Future research needs to test more types of faults and actual scenarios to improve the universality and robustness of the model.

Source of funding: *This research received no external funding.*

Declaration of competing interest: *The author declares no conflict of interest.*

REFERENCES

1. Zhang X, Zhao B, Lin Y. machine learning based bearing fault diagnosis using the case western reserve university data: A review. IEEE Access 2021; 9: 155598–608. https://doi.org/10.1109/ACCESS.2021.3128669.
2. Chen X, Zhang B, Gao D. Bearing fault diagnosis base on multi-scale CNN and LSTM model. Journal of Intelligent Manufacturing 2021; 32(4): 971–87. https://doi.org/10.1007/s10845-020-01600-2.
3. Xiao Y, Shao H, Han S, Huo Z, Wan J. Novel joint transfer network for unsupervised bearing fault diagnosis from simulation domain to experimental domain. IEEE/ASME Transactions on Mechatronics 2022; 27(6): 5254–63. https://doi.org/10.1109/TMECH.2022.3177174.
4. Li C, Li S, Zhang A, He Q, Liao Z, Hu J. Meta-learning for few-shot bearing fault diagnosis under complex working conditions. Neurocomputing 2021; 439: 197–211. https://doi.org/10.1016/j.neucom.2021.01.099.
5. Diab AAZ, Abdul-Ghaffar HI, Ahmed AA, Ramadan HA. An effective model parameter estimation of PEMFCs using GWO algorithm and its variants. IET Renewable Power Generation 2022; 16(7): 1380–400. https://doi.org/10.1049/rpg2.12359.
6. Yang J, Zhao H, Chen S. Illumination correction model with sine-cosine algorithm to optimize gray wolf population for least-squares support vector regression. Color Research & Application 2022; 47(1): 92–106. https://doi.org/10.1002/col.22716.
7. Mohammed HM, Abdul ZKh, Rashid TA, Alsadoon A, Bacanin N. A new K-means grey wolf algorithm for engineering problems. World Journal of Engineering 2021; 18(4): 630–8. https://doi.org/10.1108/WJE-10-2020-0527.
8. Djema MA, Boudour M, Agbossou K, Cardenas A, Doumbia ML. GWO-based direct power control with improved LCL filter design for three-phase inverters. International Journal of Digital Signals and Smart Systems 2021; 5(1): 3. https://doi.org/10.1504/IJDSSS.2021.112791.
9. Chen Y, Zhang D, Zhang H, Wang QG. Dual-Path Mixed-Domain Residual threshold networks for bearing fault diagnosis. IEEE Transactions on Industrial Electronics 2022; 69(12): 13462–72. https://doi.org/10.1109/TIE.2022.3144572.
10. Gao S, Xu L, Zhang Y, Pei Z. Rolling bearing fault diagnosis based on SSA optimized self-adaptive DBN. ISA Transactions 2022; 128: 485–502. https://doi.org/10.1016/j.isatra.2021.11.024.
11. Tao H, Qiu J, Chen Y, Stojanovic V, Cheng L. Unsupervised cross-domain rolling bearing fault diagnosis based on time-frequency information fusion. Journal of the Franklin Institute 2023; 360(2): 1454–77. https://doi.org/10.1016/j.jfranklin.2022.11.004.
12. Cui B, Weng Y, Zhang N. A feature extraction and machine learning framework for bearing fault diagnosis. Renewable Energy 2022; 191: 987–97. https://doi.org/10.1016/j.renene.2022.04.061.
13. Ding J, Wang Z, Yao L, Cai Y. Rolling bearing fault diagnosis based on GCMWPE and parameter optimization SVM. Zhongguo Jixie Gongcheng/China Mechanical Engineering 2021; 32: 147–55. https://doi.org/10.3969/j.issn.1004-132X.2021.02.004.
14. Rizal A, Priharti W, Rahmawati D, Mukhtar H. Classification of pulmonary crackle and normal lung sound using spectrogram and support vector machine. Journal of Biomimetics, Biomaterials and Biomedical Engineering 2022;55:143–53. https://doi.org/10.4028/p-tf63b7.
15. Ünver M, Olgun M, Department of Mathematics, Ankara University, Türkiye, Türkarslan E, Department of Mathematics, TED University, Türkiye. Cosine and Cotangent Similarity Measures Based on Choquet Integral for Spherical Fuzzy Sets and Applications to Pattern Recognition. Journal of Computational and Cognitive Engineering 2022; 1(1): 21–31. https://doi.org/10.47852/bonviewJCCE2022010105.
16. Maji A, Mukherjee I. An unsupervised one-class-classifier support vector machine to simultaneously monitor location and scale of multivariate quality characteristics. International Journal of Quality &

Reliability Management 2023; 40(2): 419–54. https://doi.org/10.1108/IJQRM-09-2021-0316.
17. Xie Q, Guo Z, Liu D, Chen Z, Shen Z, Wang X. Optimization of heliostat field distribution based on improved Gray Wolf optimization algorithm. Renewable Energy. 2021;176:447–58. https://doi.org/10.1016/j.renene.2021.05.058.
18. Sharma S, Kapoor A. An efficient routing algorithm for iot using gwo approach: International Journal of Applied Metaheuristic Computing 2021; 12(2): 67–84. https://doi.org/10.4018/IJAMC.2021040105.
19. Gul F, Rahiman W, Alhady SSN, Ali A, Mir I, Jalil A. Meta-heuristic approach for solving multi-objective path planning for autonomous guided robot using PSO–GWO optimization algorithm with evolutionary programming. Journal of Ambient Intelligence and Humanized Computing 2021; 12(7): 7873–90. https://doi.org/10.1007/s12652-020-02514-w.
20. Indramaya E, Suyanto S. Comparative study of recent swarm algorithms for continuous optimization. Procedia Computer Science 2021; 179: 685–95. https://doi.org/10.1016/j.procs.2021.01.056.

Lingbo JIANG
B.S. in Information and Computing Science, Shandong University of Technology in 2003, M.S. in Solid Mechanics, Shandong University of Technology in 2006. Research Direction: Mechanical Structure Optimization.
Work Experience: 2006-present, Teacher of School of Mechanical and Electrical Engineering, Shandong Vocational College of Industry.
Academic situation: Published 12 academic papers, participated in 4 research projects, 3 utility model patents.